Effect of inertia on the insoluble-surfactant instability of a shear flow

Alexander L. Frenkel and David Halpern
Department of Mathematics, University of Alabama, Tuscaloosa, Alabama 35487, USA
(Received 14 September 2004; published 6 January 2005)

We study, for the case of the two-layer plane Couette flow, the effects of inertia on the recently found instability due to insoluble surfactants. The insoluble-surfactant instability takes place even when inertia is absent provided an interface or a free surface under a nonzero shear is laden with an insoluble surfactant. Considering a normal mode of the streamwise wave number α, the perturbation theory we construct is good for any α provided the Reynolds number is correspondingly small. Inertia is responsible for some notable effects, including the appearance of new regions of instability and stability. For long—and only for long—waves, the following growth-rate additivity property for the inertia and interfacial instabilities holds: the growth rate corresponding to some nonzero values of the Marangoni number M and the Reynolds number Re is the sum of two contributions, one corresponding to the same value of M but zero Re, and the other corresponding to the same (nonzero) Re but zero M. This violation of the additivity property is in contrast to the case of a surfactantless Couette flow where this property holds for all wave numbers. Thus these results provide a counterexample to a conjecture that this additivity property is a universal principle. Among other results, when the thiner layer is the less viscous one, there is a nonzero critical Marangoni number M_c for the onset of instability; this (long-wave) threshold M_c grows from zero with the Reynolds number. Also, varying the ratio of viscosities through certain characteristic values leads to changes in the topology of marginal-stability curves.

DOI: 10.1103/PhysRevE.71.016302 PACS number(s): 47.20.Ft, 47.20.Ma, 47.20.Dr, 47.15.Gf

I. INTRODUCTION

Two-layer flows including those containing surfactants occur in many industrial and biomedical situations—such as coating in photography (e.g., [1]), the closure of the small airways of the lungs in which the air normally flows in contact with the liquid lining the walls (e.g., [2,3]), lubricated pipelining (e.g., [4]), and secondary oil recovery (e.g., [5]). Clearly, stability of such flows is of considerable interest.

It is well known since the work of Yih [6] that the shear flow of two fluids with different viscosities can be unstable. In the leading order, the Stokes-flow approximation, the channel flow is neutrally stable; the instability appears in the next order (of the perturbative expansion in a small long-wave parameter) which captures the effect of inertia (reflected in the dependence of the stability properties on the Reynolds number). Thus, this instability is due to the effects of inertia.

Recently, in Refs. [7] and [8], we found that even the Stokes-flow (stable in the absence of surfactants) regimes can be unstable if an insoluble surfactant is present and the interfacial shear rates are nonzero (see also Ref. [9]). In contrast to the solely long-wave treatment of Yih [6] (which required only simple polynomial eigenfunctions), but similar to, e.g., Jain and Rukenstein [10], Ref. [8] noticed that the spanwise structure of a normal mode having arbitrary streamwise length is a finite linear combination of certain functions (which are products of power and hyperbolic functions). Hence, the originally differential-equation eigenvalue problem is reduced to an algebraic one, and the growth rates are found by solving a quadratic equation whose coefficients are known elementary functions of the parameters. This allowed us in Ref. [8] to readily investigate the Stokes-flow stability properties for all wavelengths, over the entire parameter space.

Naturally, these (Stokes-flow) properties do not depend on the Reynolds number. However, such a dependence should be recovered when the next order (inertia) correction to the Halpern and Frenkel [8] theory is considered. This implies perturbative expansions in the small parameter which is proportional to the dimensionless wave number and the Reynolds number—each of which can be arbitrarily small or large provided the other is appropriately restricted. (The latter circumstance is in contrast to Yih [6], who, to reiterate, used expansions in the powers of a small-wave number parameter which did not involve the Reynolds number; the latter, however, was restricted to be order 1 or less.) This is how in the present communication we study the effects of inertia on the inertialess instability found in Refs. [7] and [8]. For simplicity, we consider a plane Couette flow. (For a similar treatment of inertia effects in surfactantless Couette-flow stability, see Albert and Charru [11]. They, however, used expansions in a small parameter which was just the Reynolds number and did not include the wave number factor.)

The stability of plane Couette flow of two fluids with no surfactants has been extensively studied. (For an overview and further references, see Refs. [4,11].) In contrast, there has been only a small number of stability studies for flows with insoluble surfactants. The earlier studies considered mostly single-fluid flows down inclined or vertical planes (e.g., [12–15]; see also Ref. [16]). In such flows, the surface value of the shear rate is zero. As was pointed out in Ref. [8], this might be the reason for the absence of destabilization of those flows by surfactants. Indeed, the results of that work (along with Ref. [7]) led us to conjecture there that nonzero shear at an interface or free surface is necessary for the insoluble-surfactant instability. (It follows, for example, that applying an external tangential stress to a film flowing down an inclined plane can destabilize a previously stable flow with insoluble surfactants at its free surface; however, this

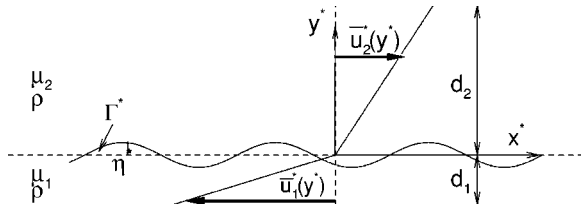

FIG. 1. Schematics of a two-layer Couette flow in the reference frame in which the basic interface, the horizontal dashed line at $y^*=0$, is at rest. The upper plate (at $y^*=d_2$) moves to the right with the speed U_2 and the lower plate (at $y^*=-d_1$) moves to the left with the speed U_1. The disturbed interface $y^*=\eta^*(x^*,t^*)$ is shown as a sinusoidal curve. $\Gamma^*(x^*,t^*)$ is the concentration of the insoluble surfactant monolayer. The velocity profile (bold arrows) is piecewise linear. μ_1 and μ_2 are the viscosities, and ρ is the common density of the two fluids.

prediction has not as yet been verified.) The interfacial shear rate is clearly nonzero for the case of the two-layer Couette flow whose insoluble-surfactant instability was uncovered in Refs. [7,8]. [The interfacial shear is also nonzero for the case of a core-annular flow studied in an unpublished work by H.H. Wei and D. Rumschitzki (private communication). However, the capillary instability of the cylindrical interface is always present, so the insoluble-surfactant instability cannot be studied in its "pure form." The crucial role of the interfacial shear first transpired in Ref. [7].] In the present communication, we choose the case of a plane (Couette) flow (a particular case of those considered in Refs. [7,8]) to study the effect of inertia on the insoluble-surfactant instability.

In Sec. II, the governing equations and the basic flow are given. In Sec. III, the stability problem is formulated. Results are presented in Sec. IV. Section V contains a summary of results and some discussions.

After the present work had been finished and submitted for publication, a related paper, Ref. [17] (an uncorrected proof), became available online. We have added a comparison of the results in appropriate places below. The subject matter is the same, but the approaches of the two papers differ; each has its own advantages. In general, they complement and support each other.

II. GOVERNING EQUATIONS AND THE BASIC STATE

The Couette flow of two immiscible fluid layers between two infinite parallel plates considered here (see Fig. 1) is a particular case of the more general Couette-Poiseuille flow treated in Refs. [7] and [8]. Therefore, we will omit some overlapping details.

Let the basic flow be driven by a shearing motion of the solid plates.

For simplicity, the densities of the two fluids are equal, and gravity is not included. (It is straightforward to generalize this formulation to include gravity, as in Ref. [9].) It is convenient to use the reference frame of the unperturbed interface. Let y^* be the spanwise, "vertical," coordinate (the symbol * indicates a dimensional quantity) measured from the basic interface ($y^*=0$) with y^* being positive in the thicker layer. We have $d_1 \leqslant d_2$, where d_1 and d_2 are the thicknesses of the "lower" and "upper" fluids, respectively. Without loss of generality, the x-directed velocity U_2 of the upper plate (at $y^*=d_2$) is positive and the velocity of the lower plate (at $y^*=-d_1$) is $-U_1$, where $U_1>0$. It is easy to see that, in terms of U, the velocity of the upper plate relative to the lower plate (i.e., $U=U_1+U_2$), we have $U_1=\mu_2 d_1(\mu_2 d_1+\mu_1 d_2)^{-1}U$ and $U_2=\mu_1 d_2(\mu_2 d_1+\mu_1 d_2)^{-1}U$, where μ_1 and μ_2 are the viscosities of the lower and upper fluids, respectively.

The well-known Squire's theorem, generalized and proved for the case with insoluble surfactants in Ref. [8], allows us to confine our consideration to the two-dimensional perturbed flows (in the x^*y^* plane). The Navier-Stokes and incompressibility equations governing the fluid motion in the two layers are (with $j=1$ for the lower layer and $j=2$ for the upper one)

$$\rho\left(\frac{\partial \boldsymbol{v}_j^*}{\partial t^*}+\boldsymbol{v}_j^*\cdot\nabla^*\boldsymbol{v}_j^*\right)=-\nabla^* p_j^*+\mu_j\nabla^{*2}\boldsymbol{v}_j^*,$$

$$\nabla^*\cdot\boldsymbol{v}_j^*=0, \tag{1}$$

where $\nabla^*=(\partial/\partial x^*,\partial/\partial y^*)$, ρ is the density (of both fluids), $\boldsymbol{v}_j^*=(u_j^*,v_j^*)$ is the fluid velocity with horizontal component u_j^* and vertical component v_j^*, and p_j^* is the pressure.

We use the "no-slip, no-penetration" boundary conditions (requiring zero relative velocities) at the plates: $u_1^*=-U_1$, $v_1^*=0$ at $y^*=-d_1$; and $u_2^*=U_2$, $v_2^*=0$ at $y^*=d_2$. The interfacial boundary conditions are as follows. The velocity must be continuous at the interface $y^*=\eta^*(x^*,t^*)$: $[\boldsymbol{v}^*]_1^2=0$, where $[A]_1^2=A_2-A_1$ denotes the jump in A across the interface. The interfacial balances of the tangential and normal stresses are, respectively,

$$\frac{1}{1+\eta_{x^*}^{*2}}[(1-\eta_{x^*}^{*2})\mu(u_{y^*}^*+v_{x^*}^*)+2\eta_{x^*}^{*2}\mu(v_{y^*}^*-u_{x^*}^*)]_1^2 = -\frac{\sigma_{x^*}^*}{(1+\eta_{x^*}^{*2})^{1/2}}, \tag{2}$$

$$\left\{(1+\eta_{x^*}^{*2})p^*-2\mu[\eta_{x^*}^{*2}u_{x^*}^*-\eta_{x^*}^*(u_{y^*}^*+v_{x^*}^*)+v_{y^*}^*]\right\}_1^2 = \frac{\eta_{x^*x^*}^*}{(1+\eta_{x^*}^{*2})^{1/2}}\sigma^*, \tag{3}$$

where σ^* is the surface tension which depends on the surface concentration of the insoluble surfactant Γ^*, and the subscripts indicate partial derivatives. The kinematic condition is $\eta_{t^*}^*=v^*-u^*\eta_{x^*}^*$. The surface concentration equation (as was derived in Ref. [8]) is

$$\frac{\partial(H\Gamma^*)}{\partial t^*}+\frac{\partial}{\partial x^*}(H\Gamma^* u^*)=D_s\frac{\partial}{\partial x^*}\left(\frac{1}{H}\frac{\partial\Gamma^*}{\partial x^*}\right), \tag{4}$$

where $H=\sqrt{1+\eta_x^{*2}}$, and D_s is the surface molecular diffusivity of surfactant; D_s is usually negligible, and is discarded below. For the linear stability problem we are interested in, we can linearize the surface tension dependence on the sur-

factant concentration: $\sigma^*=\sigma_0-E(\Gamma^*-\Gamma_0)$, where σ_0 is the basic surface tension and E is a constant.

We introduce the dimensionless variables

$$(x,y)=\frac{(x^*,y^*)}{d_1},\quad t=\frac{t^*}{d_1\mu_1/\sigma_0},\quad (u,v)=\frac{(u^*,v^*)}{\sigma_0/\mu_1},$$

$$p=\frac{p^*}{\sigma_0/d_1},\quad \Gamma=\frac{\Gamma^*}{\Gamma_0},\quad \sigma=\frac{\sigma^*}{\sigma_0}. \tag{5}$$

The dimensionless velocity field of the basic Couette flow, with a flat interface, $\eta=0$; no pressure, $\bar{p}=0$; and uniform concentration of surfactant, $\bar{\Gamma}=1$ (where the overbar indicates a basic state quantity), is the following (linear) solutions of the governing equations:

$$\bar{u}_1(y)=sy,\quad \bar{v}_1=0\quad \text{for } -1\leqslant y\leqslant 0, \tag{6}$$

$$\bar{u}_2(y)=\frac{s}{m}y,\quad \bar{v}_2=0\quad \text{for } 0\leqslant y\leqslant n, \tag{7}$$

where $1\leqslant n=d_2/d_1$ and $m=\mu_2/\mu_1$. Here the constant s, the dimensionless shear rate, is proportional to the relative plate speed: $s=[m/(m+n)]U\mu_1/\sigma_0=U_1\mu_1/\sigma_0$. Note that, due to the measurement units, the shear parameter s is equal to the capillary number, $\mathrm{Ca}=\mu_1U_1/\sigma_0$,

$$s=\mathrm{Ca},$$

although they are defined independently. For this reason, and in parallel with Ref. [17], we chose not to eliminate one of them in favor of the other.

III. STABILITY PROBLEM FORMULATION

The general formulation of the linear stability problem for the two-dimensional infinitesimal disturbances has been given in Ref. [7]. For convenience, an abridged account is included below.

We consider the perturbed state with small deviations from the basic flow: $\eta=\tilde{\eta}$, $u_j=\bar{u}_j+\tilde{u}_j$, $v_j=\tilde{v}_j$, $p_j=\tilde{p}_j$, and $\Gamma=1+\tilde{\Gamma}$. We introduce disturbance stream functions $\tilde{\psi}_j$ whose derivatives are the components of velocity: $\tilde{u}_j=\tilde{\psi}_{j_y}$ and $\tilde{v}_j=-\tilde{\psi}_{j_x}$. The normal modes have the form

$$(\tilde{\eta},\tilde{\psi}_j,\tilde{p}_j,\tilde{\Gamma})=[h,\phi_j(y),f_j(y),g]\mathrm{e}^{\mathrm{i}\alpha(x-ct)}, \tag{8}$$

where α is the wave number of the disturbance, g and h are constants, and $c=c_R+\mathrm{i}c_I$ is the complex wave-speed. The growth rate γ depends on the imaginary part of c only: $\gamma=\alpha c_I$. Linearizing the kinematic boundary condition yields $\tilde{\eta}_t(x,t)=-\tilde{\psi}_x(x,0,t)$. Hence h is expressed in terms of the stream-function,

$$h=\phi_1(0)/c \tag{9}$$

(assuming $c\neq 0$). The momentum equations can be cast as the well-known Orr-Sommerfeld equations for the stream-functions,

$$m_j(D^2-\alpha^2)^2\phi_j=\mathrm{i}\alpha\frac{\mathrm{Re}}{\mathrm{Ca}}[(\bar{u}_j-c)(D^2-\alpha^2)\phi_j-\phi_jD^2\bar{u}_j], \tag{10}$$

where $m_1=1$, $m_2=m$, $D=\mathrm{d}/\mathrm{d}y$, and $\mathrm{Re}=\rho U_1d_1/\mu_1$ is the Reynolds number.

The disturbance stream-functions ϕ_j are subject to the boundary conditions at the plates and at the interface. The boundary conditions at the plates require

$$\phi_1(-1)=\phi_1'(-1)=\phi_2(n)=\phi_2'(n)=0, \tag{11}$$

where the prime indicates differentiation with respect to y. Continuity of velocity at the interface implies

$$\phi_1(0)=\phi_2(0) \tag{12}$$

and

$$m[\phi_1'(0)-\phi_2'(0)]=(1-m)\frac{s}{c}\phi_1(0). \tag{13}$$

After linearization, the normal stress condition, Eq. (3), yields

$$m\phi_2'''(0)-\phi_1'''(0)-3\alpha^2[m\phi_2'(0)-\phi_1'(0)]=-\mathrm{i}\frac{\alpha^3}{c}\phi_2(0). \tag{14}$$

The linearized tangential stress condition, Eq. (2), reads $m\phi_2''(0)-\phi_1''(0)+\alpha^2[m\phi_2(0)-\phi_1(0)]=\mathrm{i}M\alpha g$, where $M=E\Gamma_0/\sigma_0$ is the Marangoni number. We replace the constant g in this equation by its expression from the linearized surfactant transport equation [derived from Eq. (4)], $\tilde{\Gamma}_t+\bar{u}_{1_y}(0)\tilde{\eta}_x+\tilde{\psi}_{1_{xy}}(x,0,t)=0$, whence $g=(1/c)\phi_1'(0)+(s/c^2)\phi_1(0)$. As a result, the linearized tangential-stress balance condition is written purely in terms of stream-functions,

$$m\phi_2''(0)-\phi_1''(0)+\alpha^2[m\phi_2(0)-\phi_1(0)]=\mathrm{i}M\frac{\alpha}{c}\left[\phi_1'(0)+\frac{s}{c}\phi_1(0)\right]. \tag{15}$$

In the present work, to study the effect of inertia [mathematically the nonzero right-hand side of Eq. (10)], we expand (cf. the expansions of Ref. [18], which studied a single-fluid Couette flow) the stream-functions and the complex wavespeed as

$$\phi_j(y)=\phi_{j0}(y)+\mathrm{i}\varepsilon\phi_{j1}(y),\quad c=c_0+\mathrm{i}\varepsilon c_1, \tag{16}$$

where $\varepsilon=\alpha\,\mathrm{Re}/\mathrm{Ca}$. The eigenfunctions ϕ_{j0}, the solutions of the problem with the (Stokes-) simplified Orr-Sommerfeld equations

$$(D^2-\alpha^2)^2\phi_{j0}=0, \tag{17}$$

are known for arbitrary wave numbers from Ref. [8] (where the present ϕ_{j0} were denoted simply as ϕ_j), together with the eigenvalue c_0 (a modified notation for the wavespeed c of Ref. [8]).

The inertia corrections $\phi_{j1}(y)$ satisfy the equations

$$m_j(D^2-\alpha^2)^2\phi_{j1}=[(\bar{u}_j-c_0)(D^2-\alpha^2)\phi_{j0}-\phi_{j0}D^2\bar{u}_j], \tag{18}$$

where, assuming

$$\left|\frac{\varepsilon\phi_{j1}}{\phi_{j0}}\right|\ll 1, \quad \left|\frac{\varepsilon c_1}{c_0}\right|\ll 1, \tag{19}$$

we have changed ϕ_j to ϕ_{j0} and c to c_0 on the right-hand side of Eq. (18). The last term of Eq. (18) disappears for the case of a Couette flow, and one looks for the general solution in the form

$$\begin{aligned}\phi_{j1}(y)=&B_{j1}\sinh(\alpha y)+C_{j1}y\cosh(\alpha y)+D_{j1}y\sinh(\alpha y)\\&+E_{j1}y^2\cosh(\alpha y)+F_{j1}y^2\sinh(\alpha y)\\&+G_{j1}y^3\cosh(\alpha y)+H_{j1}y^3\sinh(\alpha y).\end{aligned} \tag{20}$$

The first three terms are homogeneous solutions; they vanish when Eq. (20) is substituted into Eq. (18). Then the coefficients E_{j1}, F_{j1}, G_{j1}, and H_{j1} are readily obtained using the already known expressions for the quantities appearing on the right-hand side of Eq. (18). They are

$$\begin{aligned}E_{11}=&-\frac{\alpha s+ss_\alpha c_\alpha+\alpha c_0c_\alpha^2}{4\alpha^3}\\&+\frac{ss_\alpha^2+\alpha c_0(-\alpha+s_\alpha c_\alpha)}{4\alpha^3}B_{10},\end{aligned} \tag{21}$$

$$F_{11}=-\frac{sc_\alpha^2+\alpha c_0(\alpha+s_\alpha c_\alpha)}{4\alpha^3}+\frac{-\alpha s+ss_\alpha c_\alpha+\alpha c_0s_\alpha^2}{4\alpha^3}B_{10}, \tag{22}$$

$$G_{11}=\frac{sc_\alpha^2}{12\alpha^2}+\frac{s(\alpha-s_\alpha c_\alpha)}{12\alpha^2}B_{10}, \tag{23}$$

$$H_{11}=\frac{s(\alpha+s_\alpha c_\alpha)}{12\alpha^2}-\frac{ss_\alpha^2}{12\alpha^2}B_{10}, \tag{24}$$

$$\begin{aligned}E_{21}=&\frac{\alpha ns+ss_{\alpha n}c_{\alpha n}-\alpha mc_0c_{\alpha n}^2}{4\alpha^3m^2n^2}\\&+\frac{ss_{\alpha n}^2+\alpha c_0m(\alpha n-s_{\alpha n}c_{\alpha n})}{4\alpha^3m^2n^2}B_{20},\end{aligned} \tag{25}$$

$$\begin{aligned}F_{21}=&\frac{-sc_{\alpha n}^2+\alpha mc_0(\alpha m+s_{\alpha n}c_{\alpha n})}{4\alpha^3m^2n^2}\\&+\frac{\alpha ns-ss_{\alpha n}c_{\alpha n}+\alpha mc_0s_{\alpha n}^2}{4\alpha^3m^2n^2}B_{20},\end{aligned} \tag{26}$$

$$G_{21}=\frac{sc_{\alpha n}^2}{12\alpha^2m^2n^2}-\frac{s(\alpha n-s_{\alpha n}c_{\alpha n})}{12\alpha^2m^2n^2}B_{20}, \tag{27}$$

and

$$H_{21}=\frac{-s(\alpha n+s_{\alpha n}c_{\alpha n})}{12\alpha^2m^2n^2}-\frac{ss_{\alpha n}^2}{12\alpha^2m^2n^2}B_{20}, \tag{28}$$

where we have used the abbreviations

$$c_\alpha=\cosh(\alpha),\ s_\alpha=\sinh(\alpha),$$

$$c_{\alpha n}=\cosh(\alpha n),\ s_{\alpha n}=\sinh(\alpha n). \tag{29}$$

Here (see Ref. [8]; note that our B_{j0} are their B_j) $B_{10}=mB_{20}-\mathrm{i}/2c_0$; the coefficient B_{20} is found in terms of c_0 from the equation

$$\begin{aligned}&\left[(m-1)\alpha-\frac{ms_\alpha^2}{\alpha}+\frac{s_{\alpha n}^2}{\alpha n^2}\right]B_{20}+\left[\left(1-\frac{1}{m}\right)s-\frac{\mathrm{i}}{2}\left(\alpha-\frac{s_\alpha^2}{\alpha}\right)\right]\frac{1}{c_0}\\&+\frac{n+1}{n}+\frac{1}{\alpha}\left(s_\alpha c\alpha+\frac{s_{\alpha n}c_{\alpha n}}{n^2}\right)=0,\end{aligned} \tag{30}$$

and c_0 solves the quadratic equation

$$q_2c_0^2+q_1c_0+q_0=0. \tag{31}$$

The coefficients q_0, q_1, and q_2 are

$$q_0=\frac{1}{4}\frac{M}{\alpha}(\alpha^2n^2-s_{\alpha n}^2)(\alpha^2-s_\alpha^2)-\frac{\mathrm{i}}{2}Ms(s_{\alpha n}^2-s_\alpha^2n^2), \tag{32}$$

$$\begin{aligned}q_1=&(m-1)s(\alpha n^2-n^2s_\alpha c_\alpha+\alpha n-s_{\alpha n}c_{\alpha n})\\&+\frac{\mathrm{i}}{2}\Bigg[(\alpha n+s_{\alpha n}c_{\alpha n})\left(\alpha-\frac{s_\alpha^2}{\alpha}\right)mM\\&+(\alpha^2n^2-s_{\alpha n}^2)\left(1+\frac{s_\alpha c_\alpha}{\alpha}\right)M\\&-(\alpha n-s_{\alpha n}c_{\alpha n})\left(\alpha-\frac{s_\alpha^2}{\alpha}\right)m\\&-(\alpha^2n^2-s_{\alpha n}^2)\left(1-\frac{s_\alpha c_\alpha}{\alpha}\right)\Bigg],\end{aligned} \tag{33}$$

and

$$\begin{aligned}q_2=&\left(\alpha-\frac{s_\alpha^2}{\alpha}\right)(\alpha^2n^2+c_{\alpha n}^2)m^2+2\left(\alpha n-\alpha^3n^2-\frac{s_\alpha c_\alpha s_{\alpha n}c_{\alpha n}}{\alpha}\right)m\\&+\left(\alpha+\frac{c_\alpha^2}{\alpha}\right)(\alpha^2n^2-s_{\alpha n}^2).\end{aligned} \tag{34}$$

From the boundary condition at the plates (11), taking into account the corresponding leading-order equations (see Ref. [8])

$$\phi_{10}(-1)=\phi_{10}'(-1)=\phi_{20}(n)=\phi_{20}'(n)=0, \tag{35}$$

we obtain the conditions

$$\phi_{11}(-1)=\phi_{11}'(-1)=\phi_{21}(n)=\phi_{21}'(n)=0. \tag{36}$$

Hence, the coefficients C_{j1} and D_{j1} are eliminated by being expressed in terms of B_{j1}. Then the substitution of the ϕ_{j1} into the ε corrections to the interfacial boundary conditions (13)–(15) yield (similarly to Ref. [8]) the following system of three nonhomogeneous linear equations for the three un-

knowns B_{11}, B_{21}, and c_1 [cf. Eqs. (3.16)–(3.18) of Ref. [8]]:

$$\left(\alpha - \frac{s_\alpha^2}{\alpha}\right)B_{11} + \left(-\alpha + \frac{s_{\alpha n}^2}{\alpha n^2}\right)B_{21} + \frac{(1-m)s}{m}\frac{c_1}{c_0^2} = f_1, \tag{37}$$

$$2B_{11} - 2mB_{21} - \mathrm{i}\frac{c_1}{c_0^2} = \frac{f_2}{\alpha^3}, \tag{38}$$

$$\left(\frac{\mathrm{i}M}{c_0}(s_\alpha^2 - \alpha^2) - 2(\alpha - s_\alpha c_\alpha)\right)B_{11} + \frac{2m}{n^2}(-\alpha n + s_{\alpha n}c_{\alpha n})B_{21} + \mathrm{i}M\left(\alpha + 2\alpha\frac{s}{c_0} + s_\alpha c_\alpha + (\alpha^2 - s_\alpha^2)B_{10}\right)\frac{c_1}{c_0^2} = f_3, \tag{39}$$

where

$$f_1 = \left(-1 + \frac{s_\alpha c_\alpha}{\alpha}\right)E_{11} + \left(-n + \frac{s_{\alpha n}c_{\alpha n}}{\alpha}\right)E_{21} - \frac{sa^2}{\alpha}F_{11} + \frac{s_{\alpha n}^2}{\alpha}F_{21} + \left(1 - \frac{2s_\alpha c_\alpha}{\alpha}\right)G_{11} + \left(-n + 2\frac{s_{\alpha n}c_{\alpha n}}{\alpha}\right)nG_{21} + 2\frac{s_\alpha^2}{\alpha}H_{11} + 2n\frac{s_{\alpha n}^2}{\alpha}H_{21}, \tag{40}$$

$$f_2 = 6(\alpha F_{11} - \alpha m F_{21} + G_{11} - mG_{21}), \tag{41}$$

$$f_3 = \left(\frac{\mathrm{i}M}{c_0}(\alpha - s_\alpha c_\alpha) - 2s_\alpha^2\right)E_{11} + 2ms_{\alpha n}^2 E_{21} + \left(\frac{\mathrm{i}Ms_\alpha^2}{c_0} + 2(\alpha + s_\alpha c_\alpha)\right)F_{11} + 2m(\alpha n + s_{\alpha n}c_{\alpha n})F_{21} + \left(\frac{\mathrm{i}M}{c_0}(2s_\alpha c_\alpha - \alpha) + 4c_\alpha^2\right)G_{11} + 4mnc_{\alpha n}^2 G_{21} + 2\left(\frac{\mathrm{i}Ms_\alpha^2}{c_0} + \alpha + 2s_\alpha c_\alpha\right)H_{11} + 2mn(\alpha n + 2s_{\alpha n}c_{\alpha n})H_{21}. \tag{42}$$

We derived the above equations with the help of the computer algebra system MAPLE. We also used MAPLE to solve these algebraic equations numerically and thus find the inertia ε corrections—$\mathrm{i}\varepsilon c_1$ for the phase velocity and $\mathrm{i}\varepsilon\phi_{j1}$ for the eigenfunctions. The results are presented in the next section.

In contrast to our perturbation approach, Ref. [17] used a numerical method to solve differential equations (10). This approach is less restrictive as regards the Reynolds number. The perturbative solution provides for independent checks of the numerical code of Ref. [17]. It also leads to some questions which do not naturally arise in the other approach—such as the question about the additivity property for the growth rate discussed below. For the most part, the actual results obtained in the two papers do not overlap. We say more about this below.

IV. RESULTS

A. Long waves: Analytical results

In the long-wave limit $\alpha^2 \ll D^2$, similar to Refs. [6] and [7], we can simplify Eq. (17) to the form $D^4\phi_{j0}=0$ which has polynomial solutions found in Ref. [7]. Since the functions ϕ_{j0} are fourth-degree polynomials, the general solution for the inertial correction is a sixth-degree polynomial,

$$\phi_{j1}(y) = \tilde{B}_{j1}y + \tilde{C}_{j1}y^2 + \tilde{D}_{j1}y^3 + \tilde{E}_{j1}y^4 + \tilde{F}_{j1}y^5 + \tilde{G}_{j1}y^6 \tag{43}$$

[cf. Eq. (20)]. We find

$$\tilde{E}_{j1} = -\frac{c_0\tilde{C}_{j0}}{12m_j},$$

$$\tilde{F}_{j1} = -\frac{3c_0m_j\tilde{D}_{j0} - s\tilde{C}_{j0}}{60m_j^2},$$

$$\tilde{G}_{j1} = \frac{s\tilde{D}_{j0}}{60m_j^2} \tag{44}$$

as the long-wave analog of Eqs. (21)–(28). The boundary conditions yield the following seven linear nonhomogeneous equations for the seven unknowns $\tilde{B}_{11}$, $\tilde{B}_{21}$, $\tilde{C}_{11}$, $\tilde{C}_{21}$, $\tilde{D}_{11}$, $\tilde{D}_{21}$, and c_1 [with $\tilde{B}_{10}$, $\tilde{B}_{20}$, and c_0 known from Ref. [7] (see table 1 there)]:

$$-\tilde{B}_{11} + \tilde{C}_{11} - \tilde{D}_{11} = \frac{1}{60}(7c_0 + s)\tilde{B}_{10} - \frac{s}{60} - \frac{3c_0}{20}, \tag{45}$$

$$\tilde{B}_{11} - 2\tilde{C}_{11} + 3\tilde{D}_{11} = -\left(\frac{5}{12}c_0 + \frac{1}{15}s\right)\tilde{B}_{10} + \frac{1}{2}c_0 + \frac{1}{20}s, \tag{46}$$

$$n\tilde{B}_{21} + n^2\tilde{C}_{21} + n^3\tilde{D}_{21} = \frac{n^3(sn - 7mc_0)}{60m^2}\tilde{B}_{20} + \frac{sn^3}{60m^2} - \frac{3n^2c_0}{20m}, \tag{47}$$

$$\tilde{B}_{21} + 2n\tilde{C}_{21} + 3n^2\tilde{D}_{21} = \frac{n^2(4sn - 25mc_0)}{60m^2} + \frac{sn^2}{20m^2} - \frac{nc_0}{2m}, \tag{48}$$

$$\tilde{B}_{11} - \tilde{B}_{21} + \mathrm{i}\frac{(1-m)s}{mc_0^2}c_1 = 0, \tag{49}$$

$$3\alpha^2(\tilde{B}_{11} - m\tilde{B}_{21}) - 6\tilde{D}_{11} + 6m\tilde{D}_{21} + \frac{\alpha^3}{c_0^2}c_1 = 0, \tag{50}$$

$$-\frac{\mathrm{i}M\alpha}{c_0}\tilde{B}_{11}-2\tilde{C}_{11}+2m\tilde{C}_{21}-\frac{M\alpha}{c_0^2}\left(\tilde{B}_{10}+2\frac{s}{c_0}\right)c_1=0. \tag{51}$$

We find that the ε correction does not affect the stability of the "mode 1" of Frenkel and Halpern [7] (which can be called the "surfactant mode" since it vanishes with the Marangoni number,

$$c_0=-\frac{1}{4}\frac{\mathrm{i}M(n-1)}{m-1}\alpha$$

Since the wavespeed correction $\mathrm{i}\varepsilon c_1$ is purely real,

$$\mathrm{i}\varepsilon c_1=\frac{\varepsilon}{480}\frac{(n-1)(3mn^4+4m^3n+4n^5+n^6+m^3+3m^2n^2)Ms}{(n^2-m)(n+1)(m-1)m^2}\alpha. \tag{52}$$

For the other, "nonsurfactant mode"—which is continuously connected to the sole mode of Yih [6]—the ε correction to the growth rate of the Frenkel and Halpern [7] insoluble-surfactant instability is exactly equal to the growth rate of the Yih [6] viscosity-jump instability: c_0 and the correction $\mathrm{i}\varepsilon c_1$ are given by

$$c_0=\frac{-2(m-1)(n+1)n^2s}{\psi}-\frac{\mathrm{i}(m-n^2)\varphi M}{4(m-1)\psi}\alpha \tag{53}$$

and

$$\begin{aligned}\mathrm{i}\varepsilon c_1=&-\frac{\mathrm{i}\varepsilon}{60\psi^3m^2}(4nm^2+m^2+6n^2m+4n^3+n^4)(m-1)n^2s^2\\&\times(n^8+4mn^7+8m^2n^6-2n^6m+8n^5m^2\\&-4n^5m+4n^3m^3-8n^3m^2\\&-8n^2m^2+2n^2m^3-4nm^3-m^4),\end{aligned} \tag{54}$$

where $\varphi=m+3mn+3n^2+n^3$ and $\psi=m^2+4mn+6mn^2+4mn^3+n^4$. Thus, for the long-wave case, the growth rate is the sum of independent contributions of the two instabilities, one due to viscosity stratification and the other to the insoluble surfactant: $\gamma(M,\mathrm{Re})=\gamma(M,0)+\gamma(0,\mathrm{Re})$.

This prediction made for the long-wave modes, which can be called a "growth-rate additivity property," is confirmed in the long-wave limit of the general-case, arbitrary-α results presented below. On the other hand, for the shorter-wave modes, the growth-rate additivity property breaks down, as we discuss next. This question arises naturally in the perturbation theory (but not in a numerical study such as that of Ref. [17]).

B. Computer-aided results for arbitrary wave numbers

The above statements regarding the additivity property for the growth rate are illustrated by Fig. 2. It shows that the dispersion curve for given nonzero values of Marangoni and Reynolds numbers (M,Re) is asymptotic to the sum of the two growth rates, one for the values (0,Re) and the other for (M,0), as the wave number approaches zero. However, the two curves diverge as the wave number increases. This is the case for both the nonsurfactant and surfactant modes.

One has to make sure that the consistency conditions (19) are satisfied. Estimating the order of magnitude of ϕ_{j1} in terms of ϕ_{j0} from Eq. (18), and taking into account the estimates for D^2 which follow from Eq. (20), viz., $D^2\sim 1$ for $j=1$ and $\alpha\lesssim 1$, $D^2\sim\alpha^2$ for $j=1$ and $\alpha\gg 1$, $D^2\sim n^{-2}$ for $j=2$ and $\alpha\lesssim n^{-1}$, and $D^2\sim\alpha^2$ for $j=2$ and $\alpha\gg n^{-1}$, the validity conditions (19) become

$$\left|\alpha\frac{\mathrm{Re}}{s}\frac{\max(c_0,s)}{\max(1,\alpha^2)}\right|\ll 1 \tag{55}$$

and

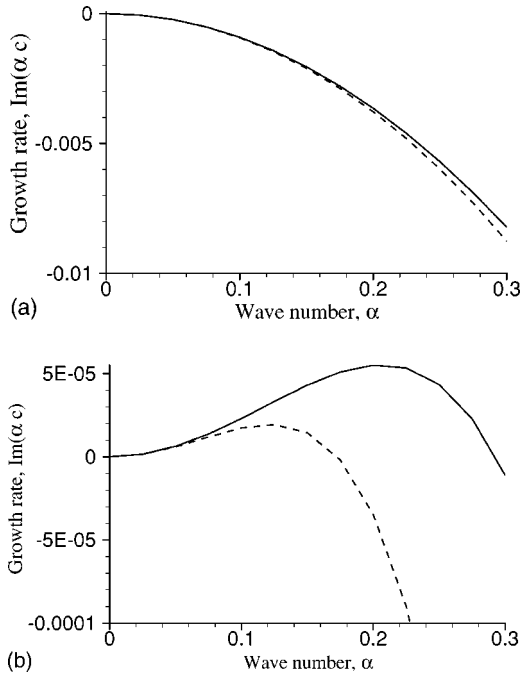

FIG. 2. Dispersion curves for $n=2$, $m=3.75$, and $s=\mathrm{Ca}=2$, for the two normal modes: (a) the nonsurfactant mode and (b) the surfactant mode. The solid lines show the growth rate $\gamma(M,\mathrm{Re})$ for $(M,\mathrm{Re})=(1,0.3)$. For comparison, the dashed lines show the sum of two growth rates, $\gamma(0,0.3)+\gamma(1,0)$.

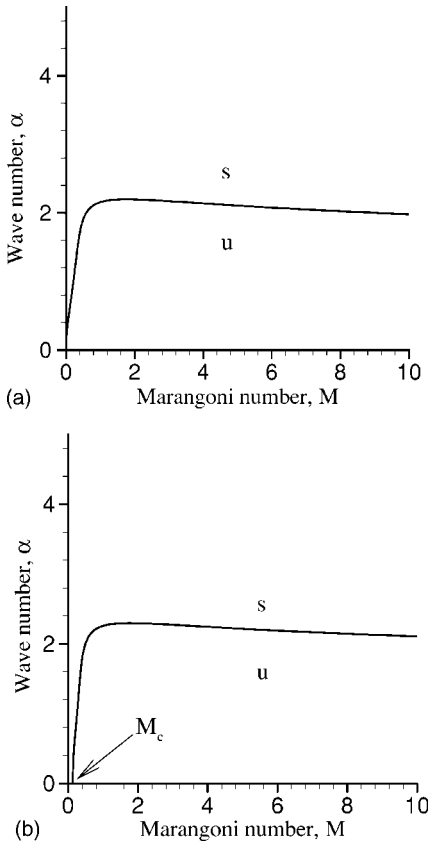

FIG. 3. Marginal stability curves for $n=3$, $m=2$, $s=\mathrm{Ca}=10$, and (a) $\mathrm{Re}=0$ and (b) $\mathrm{Re}=0.5$. "u" indicates the region of unstable normal modes and "s" corresponds to the region of stability. The nonzero critical value M_c of the Marangoni number, the M-axis intercept of the marginal curve, is due to inertia, $\mathrm{Re}\neq 0$.

$$\left|\alpha\frac{\mathrm{Re}}{s}\frac{\max(c_0,sn/m)}{m\max(n^{-2},\alpha^2)}\right|\ll 1. \tag{56}$$

We have checked that these conditions, as well as the condition $|\varepsilon c_1/c_0|\ll 1$, hold for the normal modes of Fig. 2.

Figure 3 shows how the change from the zero to a nonzero Reynolds number changes the curve of marginal stability in the wave number–Marangoni number plane. The significant effect of inertia is that the critical Marangoni number for the instability, M_c in Fig. 3(b), becomes nonzero. We have observed that M_c moves further away from zero as the Reynolds number is increased.

Figure 4 illustrates the spanwise structure of a normal mode, taking as an example the case of Fig. 3. (Because of the difference of scales, the curves corresponding to the imaginary part of the normal mode with the smaller wave number $\alpha=0.01$ are properly seen only in the blow-up shown as an inset of Fig. 4.)

For the case with $m<1$ shown in Fig. 5, the only apparent effect of inertia is the widening of the wave number range of the long-wave insoluble-surfactant instability. In particular, the marginal wave number at $M=0$, α_0, is seen to increase with the Reynolds number.

In view of the results of Ref. [8], the nonzero wave number value of the small-M limit of the marginal curve in Fig. 3(b) suggests that the mode responsible for the marginal stability is the surfactant mode. Similar considerations yield that the marginal curve in Fig. 5 corresponds to the nonsurfactant mode. We note that the questions illustrated in Figs. 2–5 are not studied in Ref. [17].

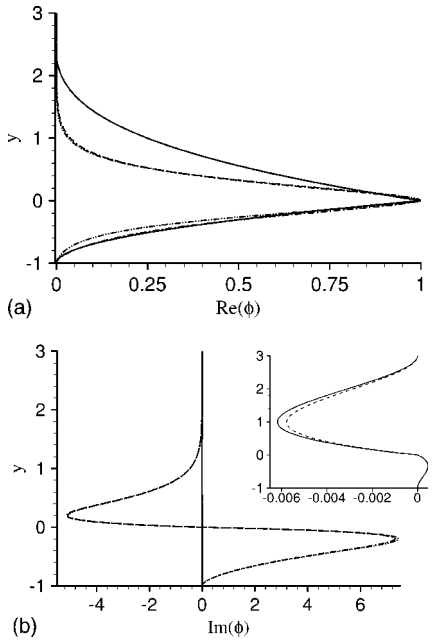

FIG. 4. The spanwise dependence of normal modes $\phi_{j0}(y)$ and $\phi_j(y)$ for $n=3$, $m=2$, $M=2$, $s=\mathrm{Ca}=10$, $\mathrm{Re}=0.5$: (a) the real parts and (b) the imaginary parts. The solid lines correspond to ϕ_{j0} for $\alpha=0.01$, the dashed lines to ϕ_j with $\alpha=0.01$, the dash-dotted lines to ϕ_{j0} with $\alpha=5$, and the dash-double-dotted lines to ϕ_j with $\alpha=5$. The inset is a blow-up of the imaginary parts for $\alpha=0.01$. Note that some of the ϕ_j curves cannot be distinguished from their ϕ_{j0} counterparts.

When inertia is taken into account, so that nonzero values of the Reynolds number Re enter consideration, one can consider the marginal stability in the α-Re plane. Figure 6 shows the effect of changing the viscosity ratio through a characteristic value, $m=n^2$, at which the two disconnected branches of the marginal curve become connected at the origin as $\mathrm{Re}_0(m)\to 0$ when $m\to n^2$, and then detach from the origin as a single smooth marginal curve. Thus, as m increases, there is a change from three to two regions of alternating stability-instability. Note that in this figure, as well as in those below, the (equal) parameters Ca and s are changing proportional to Re. This is because, along with Re, they are proportional to the basic velocity U_1, and therefore change together with Re if the material and geometrical parameters of the problem are fixed. (Note the difference with Ref. [17] where the marginal stability curves in the α-Re plane are plotted with $s=\mathrm{Ca}=\mathrm{const.}$) Figure 6(c) exhibits stability for all Reynolds numbers shown there provided the wave number is sufficiently small. Also, there is stability for all wave numbers covered provided the Reynolds number is sufficiently small.

In Fig. 7, we see a different change in the topology of the marginal curve as the viscosity ratio varies. The two branches of the marginal curve approach each other until there is one common point at which four pieces of the mar-

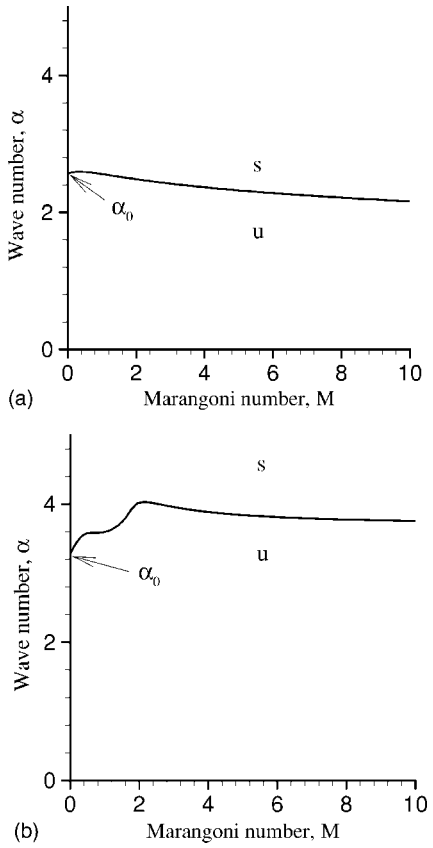

FIG. 5. Same as Fig. 3 but for a viscosity ratio value smaller than 1, viz., $m=1/3$.

ginal curve come together. Afterwards, the pieces separate again but now they are reconnected in a different arrangement. Checking the validity conditions, Eqs. (55) and (56), shows that the reconnection region is at the limit of validity for our approach. However, a similar reconnection has also been observed in Ref. [17] (see their Fig. 8). The other type of topological change, the fusion of the marginal curve, shown in our Fig. 6, has not been reported in Ref. [17] (presumably, simply because Ref. [17] did not focus its attention on the corresponding parameter range).

Finally, Fig. 8 shows a single-branch α-Re marginal curve for a case with $m<1$.

V. SUMMARY AND DISCUSSION

We have shown that the effects of inertia on the insoluble-surfactant instability are captured in successive approximations starting from the inertialess Stokes approximation, provided the Reynolds number is sufficiently (as determined by the wave number and other parameters) small. This requires considering only an algebraic eigenvalue problem which is readily solved by using no more than a computer algebra system such as MAPLE. The long-wave results are obtained analytically but a computer-aided solution is needed otherwise. In the long-wave limit, a growth-rate additivity property holds in the sense that the growth rate $\gamma(M,\mathrm{Re})$ is the sum of the two growth rates: $\gamma(M,0)+\gamma(0,\mathrm{Re})$; but, for non-small-wave numbers, this property, in general, breaks down.

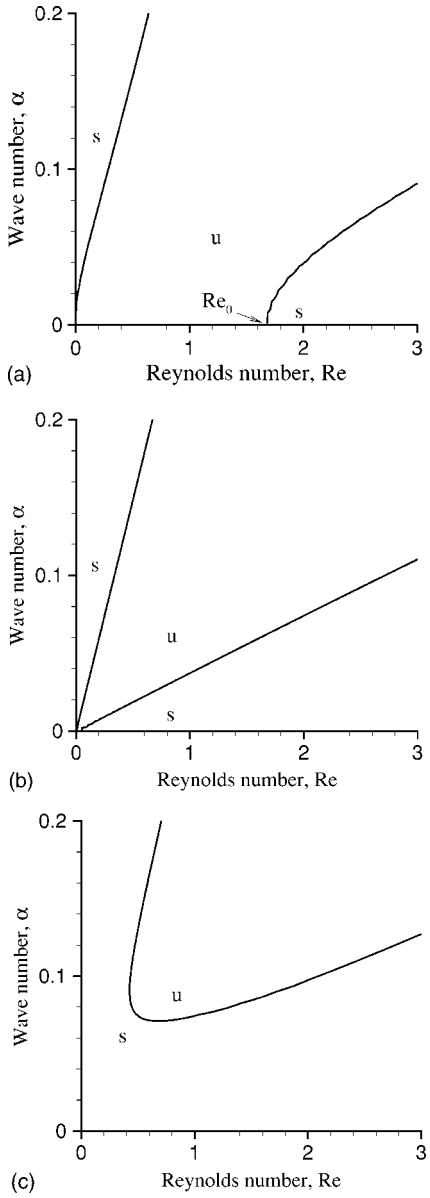

FIG. 6. Marginal stability curves for $n=1.2$, $M=1.2$, variable s and Ca such that $s/\mathrm{Re}=\mathrm{Ca}/\mathrm{Re}=2/5$, and (a) $m=1.439$, (b) $m=1.440$, and (c) $m=1.441$. The two disconnected regions of stability coalesce into one as m increases past the critical value $m=n^2$, and the two disconnected branches of the marginal curve coalesce at the origin of the α-Re plane.

This is in contrast to the surfactantless case of Ref. [11] in which this property for inertia and Rayleigh-Taylor gravity effects was found to hold for all wave numbers. If from that work one were to get an impression that this growth-rate additivity property is a universal principle, similar to the superposition principle for linear equations, then the present work gives a counterexample. Of course, the stability equations are linear, and the superposition principle involving sums of the *disturbances* holds. But the sum of the growth rates is a different matter. In general, the dispersion relation is nonlinear and gives the growth rate as a complex function of the parameters, so there is no reason to expect the additivity property for the growth rates. Also, in the long-wave

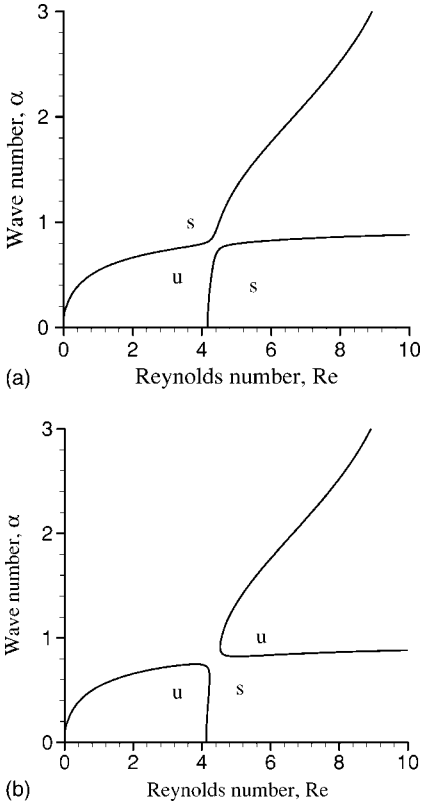

FIG. 7. Marginal stability curves for $n=2$, $M=1.1$, variable s and Ca such that $s/\mathrm{Re}=\mathrm{Ca}/\mathrm{Re}=2/5$, and (a) $m=3.29$ and (b) $m=3.3$. The topology of the marginal curve changes as m passes through a characteristic value located between 3.29 and 3.3.

limit, the first inertia correction to the growth rate (to which our consideration is confined here) is zero for the surfactant mode, but is not vanishing for the other, nonsurfactant mode (the latter is the only mode existing when no surfactants are present, as in Refs. [6] and [11]). In the limit of a clean interface, the results of Ref. [11] hold.

We have studied the change in the marginal stability curves in the wave number–Marangoni number plane as the Reynolds number is changed from zero to a nonzero value. The significant result for the viscosity ratio $m>1$ (for several values of m that we studied) is that the critical Marangoni number changes from zero to a nonzero value. Thus, the flow is stable for all wave numbers when the Marangoni number is sufficiently small. For the opposite case, $m<1$, the only change seems to be the widening of the wave number range of the long-wave instability.

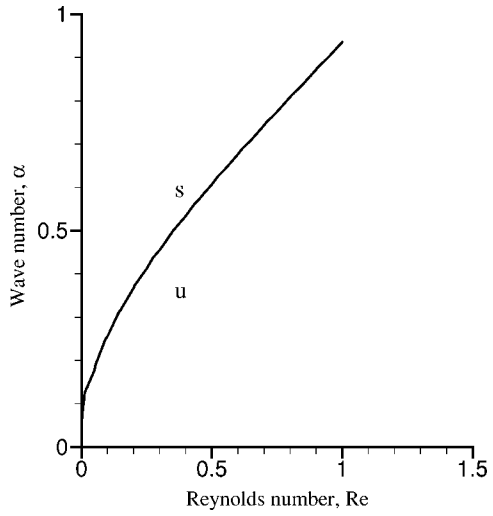

FIG. 8. Marginal curve for $n=1.2$, $M=1.2$, $m=0.5$, and $s/\mathrm{Re}=\mathrm{Ca}/\mathrm{Re}=2/5$.

When the nonzero values of the Reynolds number are brought into consideration, we can look for the marginal curves in the wave number–Reynolds number plane (which of course does not exist for the inertialess case). Varying the viscosity ratio, we have observed changes in the topology of the marginal curves at certain characteristic values. Thus, at $m=n^2$, the two branches of the marginal curve, one with the Reynolds-number intercept equal to zero and the other with a nonzero intercept Re_0, become connected as $\mathrm{Re}_0\to 0$ when $m\to n^2$. For $m>n^2$, the marginal curve detaches from the origin as a single smooth curve. As a result, for $m>n^2$, the flow is stable for all wave numbers if the Reynolds number is sufficiently small; also, it is stable for all Reynolds numbers provided the wave number is sufficiently small.

A different change in the topology of the marginal curve has been observed for larger values of m. For those, as m is increased, at some characteristic value $m_0<n^2$, the two branches come into contact at some point bounded away from the origin, and then as m is further increased, two new, reconnected marginal branches separate and move apart. This type of change of the marginal curve has also been observed in Ref. [17].

These perturbative results are subject to the validity conditions, Eq. (55) and (56). For cases in which $n\sim 1$ and $m\sim 1$, and also $c_0\lesssim s$, the two conditions simplify to become just one, $\alpha\mathrm{Re}/\max(1,\alpha^2)\ll 1$, which means $\alpha\,\mathrm{Re}\ll 1$ for $\alpha\lesssim 1$ and $\mathrm{Re}/\alpha\ll 1$ for $\alpha\gg 1$. We note that for the cases with $M=1$, there is a difficulty in satisfying the conditions (55) and (56) for large wave numbers. In Ref. [8], the short-wave asymptotic equation for c_I, the imaginary part of the wavespeed, was given, Eq. (4.14) there. (Note that there was a misprint: the last m in the first line should be M.) The two solutions were $c_I=-M/[2(m+1)]$ and $c_I=-1$. With this, Eq. (A2) of Ref. [8] yields the real part c_R, and it turns out to contain $(M-1)$ in the denominator. Thus, $|c|\to\infty$ as $M\to 1$. As a result, conditions (55) and (56) are inevitably violated. It remains an open question why the point $M=1$ should be so peculiar.

As has already been mentioned above, the numerical approach of Ref. [17] has less restrictive validity constraints. Our computer-aided approach has the advantage that it is easier to check the results and to extend the investigation to other parameter values, since one does not have to create a computer program which was necessary for the approach of Ref. [17]. We believe that the two approaches complement each other.

ACKNOWLEDGMENTS

We are grateful to Dr. M.G. Blyth and Dr. C. Pozrikidis for stimulating discussions at the early stages of both the present investigation and the work reported in Ref. [17].

[1] *Liquid Film Coating*, edited by S. F. Kistler and P. M. Schweizer (Chapman Hall, London, 1997).
[2] D. Halpern and J. B. Grotberg, J. Biomech. Eng. **115**, 271 (1993).
[3] D. R. Otis, M. Johnson, T. J. Pedley, and R. D. Kamm, J. Appl. Physiol. **75**, 1323 (1993).
[4] D. D. Joseph and Y. Renardy, *Fundamentals of Two-Fluid Dynamics, Vol 1: Mathematical Theory and Applications* (Springer, New York, 1993).
[5] J. C. Slattery, AIChE J. **20**, 1145 (1974).
[6] C. S. Yih, J. Fluid Mech. **27**, 337 (1967).
[7] A. L. Frenkel and D. Halpern, Phys. Fluids **14**, L45 (2002).
[8] D. Halpern and A. L. Frenkel, J. Fluid Mech. **485**, 191 (2003).
[9] M. G. Blyth and C. Pozrikidis, J. Fluid Mech. **505**, 59 (2004).
[10] R. K. Jain and E. Ruckenstein, J. Colloid Interface Sci. **54**, 108 (1976).
[11] F Albert and F Charru, Eur. J. Mech. B/Fluids **19**, 229 (2000).
[12] S. Whitaker, Ind. Eng. Chem. Fundam. **3**, 132 (1964).
[13] S. Whitaker and L. O. Jones, AIChE J. **12**, 421 (1966).
[14] B. E. Anshus and A. Acrivos, Chem. Eng. Sci. **22**, 389 (1967).
[15] S. P. Lin, AIChE J. **16**, 375 (1970).
[16] C. Pozrikidis, J. Fluid Mech. **496**, 105 (2003).
[17] M. G. Blyth and C. Pozrikidis, J. Eng. Math. (to be published).
[18] C. L. Pekeris, Proc. Cambridge Philos. Soc. **32**, 55 (1936).